

Study of an Energetic-oxidant Co-crystal: Preparation, Characterisation, and Crystallisation Mechanism

Han Gao, Wei Jiang*, Jie Liu, Gazi Hao, Lei Xiao, Xiang Ke, and Teng Chen

Nanjing University of Science and Technology, School of Chemical Engineering, China

**E-mail: superfine_jw@126.com*

ABSTRACT

An energetic co-crystal consisting of the most promising military explosive 2,4,6,8,10,12-hexanitro-2,4,6,8,10,12-hexaazaisowurtzitane (CL-20) and the most well-known oxidant applied in propellants ammonium perchlorate has been prepared with a simple solvent evaporation method. Scanning electron microscopy revealed that the morphology of co-crystal differs greatly from each component. The X-ray diffraction spectrum, FTIR, Raman spectra, and differential scanning calorimetry characterisation further prove the formation of the co-crystal. The result of determination of hygroscopic rate indicated the hygroscopicity was effectively reduced. At last, the crystallisation mechanism has been discussed.

Keywords: Energetic co-crystal; Ammonium perchlorate; CL-20, Solvent evaporation method; Intermolecular hydrogen bond

1. INTRODUCTION

There are three principal approaches for modification of materials used in defence technology: Improving crystal quality, ultrafine treatment and polymer coating. But these methods all have their own shortcomings like complex steps, high costs and energy reduction. Co-crystal technology are widely used for the pharmaceutical chemicals due to their functions of improving the solubility, bio-availability physical and chemical stability properties of drugs with their chemical structure unchanged¹⁻⁷, therefore, co-crystal technologies are getting more and more emphasis and applications in the field of energetic materials in recent two decades. Bolton combined the economy and the stability of TNT with the high energy density of CL-20 to form a novel co-crystal which have great charge density but lower mechanical sensitivity than CL-20⁸. Shen successfully prepared HMX/TATB co-crystal explosive by the S/NS method at room temperature. The data of impact sensitivity test indicate that the co-crystal explosive was relative insensitive in contrast to HMX⁹.

An energetic-oxidant co-crystal composed of ammonium perchlorate (AP) and 2,4,6,8,10,12-hexanitro-2,4,6,8,10,12-hexaazaisowurtzitane (CL-20) is presented here. AP is a common component of solid rocket propellant, but large water solubility, severe hygroscopicity and easy reunion, reduce the survival ability of arms¹⁰⁻¹¹. CL-20 is currently the most powerful high-energy elemental explosives used in national defense industries¹²⁻¹⁷, but high mechanical sensitivity (impact sensitivity, friction sensitivity and shock sensitivity, etc.) limits its application range¹⁸⁻²⁰. Study show that forming co-

crystal can effectively improve the solubility, dispersion and hygroscopicity of the component²¹⁻²⁵. Therefore, in order to ameliorate the hygroscopicity of AP, we consider forming co-crystal of CL-20 and AP before applying in propellant formulations.

2. EXPERIMENTAL PROCEDURE

2.1 Materials and Preparation

AP was supplied by the Dalian factory of ammonium perchlorate. ϵ -CL-20 was produced by Qingyang Chemical Industry Corporation of China. Ethanol, AR, Shanghai Lingfeng Chemical Reagent Co. Ltd.

2.2 Preparation of the Co-crystal

0.012 g AP and 0.044 g CL-20 (molar ratio 1:1) were added to 20 mL methanol. After uniformly mixing with 10 min ultrasonic oscillation, the solution was stirred for several hours and colourless and transparent crystals were obtained after 6 days volatilisation. The sample was dried through a vacuum drying process for 2 h to get CL-20/AP co-crystal.

3. CHARACTERISATIONS AND DISCUSSIONS

The samples (CL-20, AP and the co-crystal) scanning electron microscopic (SEM) morphology characterisation was observed with Hitachi S-4800. The X-ray diffraction (XRD) was carried out with a Bruker Instruments D8 Advance system in the 2θ range of 20-80° at scan rate of 0.02°/s with Cu-K_{α1} radiation ($\lambda=0.15406$ nm) operated at 40 kV and 40 mA. FT-IR and Raman spectra were determined by Thermo Fisher Nicolet iS10 FT-IR Spectrometer and HORIBA JOBIN YVON S.A.S. LABRAM Aramis, respectively. SDT Q600 was employed

to do differential scanning calorimetry (DSC) analysis. 2 mg - 3 mg sample was weighed into alumina crucible each time. Test conditions were recorded with 20 mL/min nitrogen purge flow at 20 °C /min from 25 °C to 500 °C.

3.1 SEM Studies

As shown in Fig. 1, AP crystals tend to be spherical with rounded edges and corners, which particle size is approximately 100 μm . Raw CL-20 particles are more like irregular polyhedron with uneven size. However, CL-20/AP co-crystal, presenting cubo octahedron, varies greatly from the morphology of each single component.

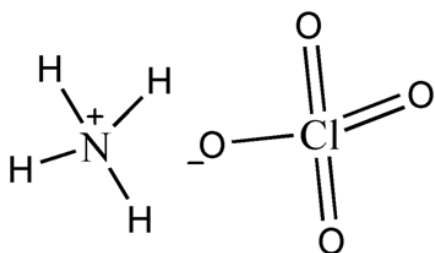


Figure 1. Structures of CL-20 and AP.

3.2 XRD Characterisation

The XRD patterns of AP, CL-20 and co-crystal are presented in Fig. 5. The characteristic peaks of AP with 2θ -values of 19.52, 22.79, 24.00, and 24.75 are not present in the co-crystal pattern. In the case of CL-20, the characteristic peaks at 10.88°, 12.74°, 13.95°, 16.46°, 25.96° and 28.02° are not present in the co-crystal. However in the co-crystal, a new peak at about 12.06°, 13.67°, 27.49° and 41.75° formed after crystallisation. The result indicated that the pattern of the as prepared co-crystal differs enormously from each individual component. The appearance of the unique powder diffraction pattern is evidence for the formation of a new crystal.

3.3 FT-IR Spectra

The FT-IR spectra of AP, CL-20 and co-crystal are as shown in Fig. 4. The assignments for the major characteristic bonds are listed in Table 1. The results indicated that several characteristic absorption peaks are highly sensitive to the structure changes of the co-crystal in the IR spectra. AP has bands at 620.00 cm^{-1} , 1411.16 cm^{-1} and 3276.47 cm^{-1} . However, these bands increased to 623.389 cm^{-1} , 1412.12 cm^{-1} and 3281.29 cm^{-1} , respectively. Similarly, some characteristic absorption peaks of CL-20 also shift after crystallisation. Those phenomena may be caused by the hydrogen bond interactions involved in co-crystal formation which changes the symmetry characteristic.

3.4 Raman Spectra

The Raman spectra of AP, CL-20 and co-crystal are presented in Fig. 5. Some characteristic peaks of AP and CL-20 are detected in the co-crystal from Micro-Raman spectroscopy (MRS). Similar to FTIR, some peak shift also take place for Raman spectra which can be attributed to intermolecular hydrogen-bonding. For example, AP has band at 3212.38 cm^{-1} and CL-20 has band at 3048.00 cm^{-1} which are $-\text{NH}$ and $-\text{CH}$

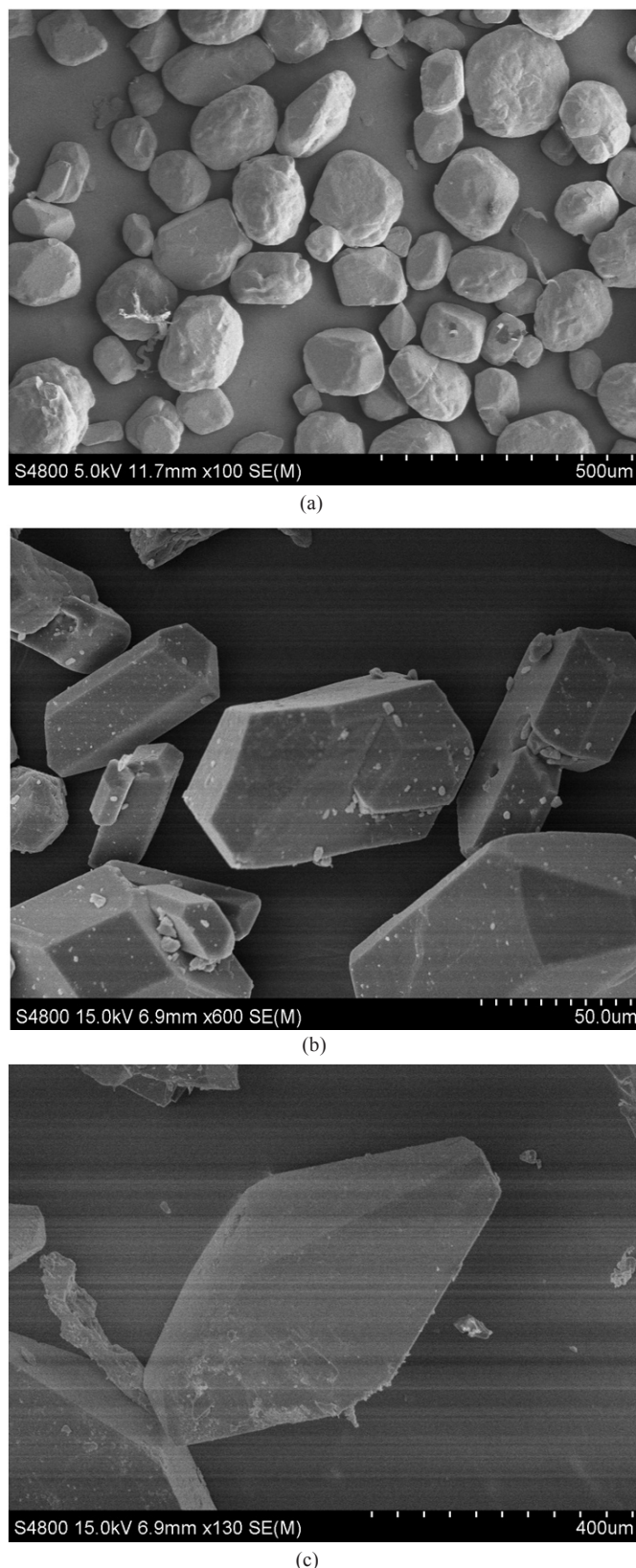
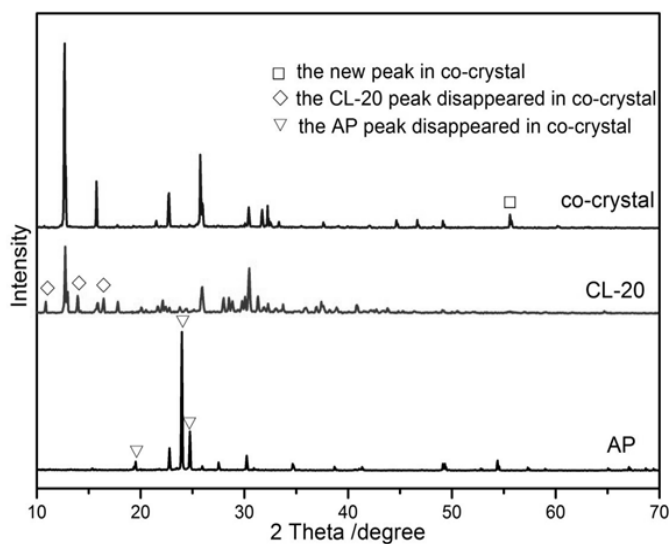
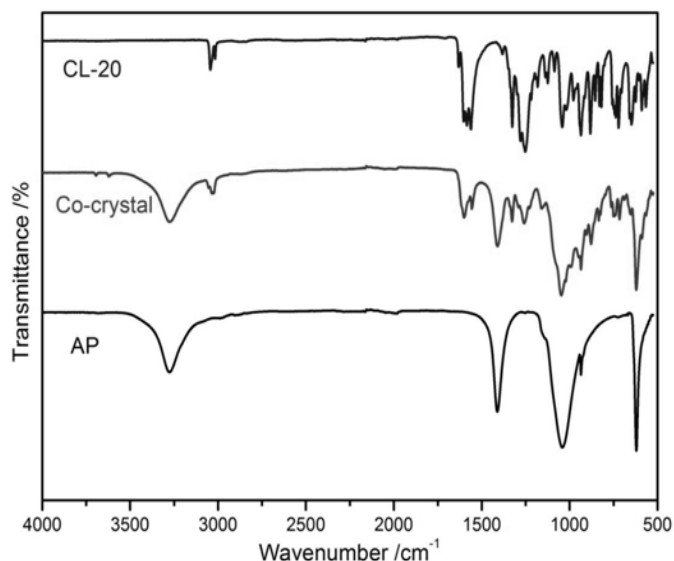
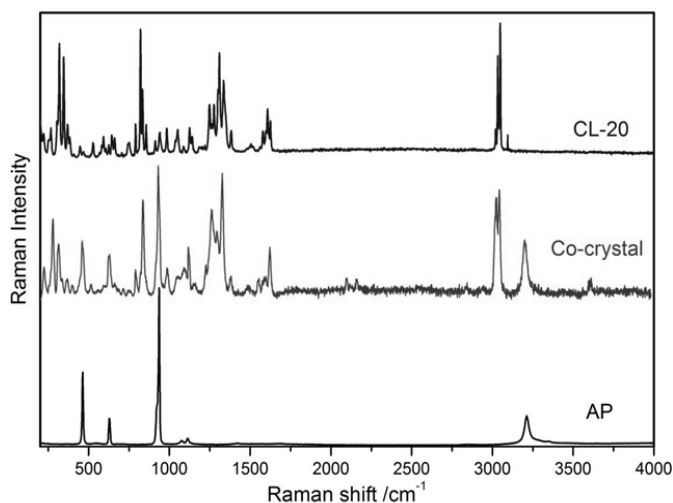


Figure 2. SEM of (a) AP, (b) CL-20, and (c) CL-20/AP co-crystal.

stretching respectively. However, these two bands shifted to 3209.30 cm^{-1} and 3054.41 cm^{-1} in the co-crystal.

Table 1. Assignments of the major bands of the FT-IR spectra of AP, CL-20, and AP/CL-20 co-crystal, cm^{-1}

Assignments	AP	Co-crystal	CL-20	Assignments
ClO_4^- stretching	620.00	623.38		
		720.76	721.25	NO_2 out-of-plane deformation
ClO_4^- stretching	935.31	935.31		
		977.73	978.21	Ring deformation
ClO_4^- stretching	1041.85	1041.85		
		1252.54	1252.06	NO_2 symmetric stretching
		1326.30	1325.82	C-H deformation
N-H bending vibration	1411.16	1412.12		
		1601.60	1602.60	NO_2 asymmetric stretching
		3016.60	3016.60	C-H stretching
		3043.12	3043.60	C-H stretching
N-H stretching	3276.47	3281.29		

**Figure 3. XRD patterns of AP, CL-20 and co-crystal.****Figure 4. FT-IR Spectrums of AP, CL-20 and co-crystal.****Figure 5. Raman Spectrums of AP, CL-20 and co-crystal.**

3.5 Thermal Property

As shown in Fig. 6, CL-20/AP co-crystal presents a unique thermal property which is different from single component CL-20 and AP. The as prepared co-crystal only has an exothermic peak at 231.3 °C, which was earlier than that of mechanical mixture at 243.8 °C. Besides, the mixture has a second exothermic peak at 282.1 °C. In Fig. 6(e), it is indicated that the co-crystal decomposed ahead of mixture, CL-20 and AP. In Fig. 7, the phenomenon is more obvious.

As shown in Fig. 7, CL-20 has only one weightless step and AP has two. This may explain why the mixture has three steps. However, the co-crystal only has two weightless steps. There's a strong interaction between CL-20 and AP. Reasons are summarised as: The decomposition temperature of CL-20 249.2 °C is close to the crystal transition peak temperature of AP 248.9 °C. A small amount of AP decomposition products (HClO_4 , ClO_3 and ClO_2 with high oxidation resistance) can affect the decomposition of CL-20. Meanwhile, the decomposition of CL-20 also influences the degradation process of AP. Compared with mechanical mixture, crystal transition peak of AP disappears and the exothermic peak

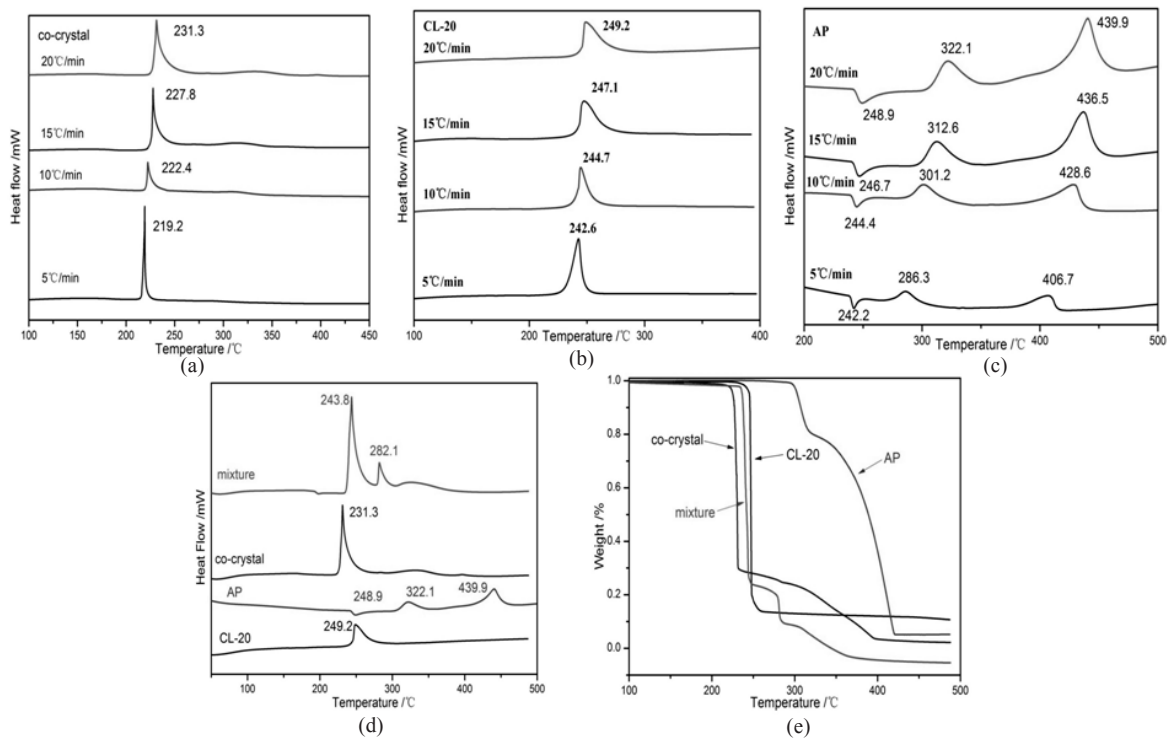


Figure 6. DSC curves of (a) CL-20/AP co-crystal, (b) CL-20, (c) AP at different heating rate, (d) DSC curves contrast of co-crystal and mechanical mixture at 20 °C/min and (e) TG curves of CL-20, AP, co-crystal and mixture.

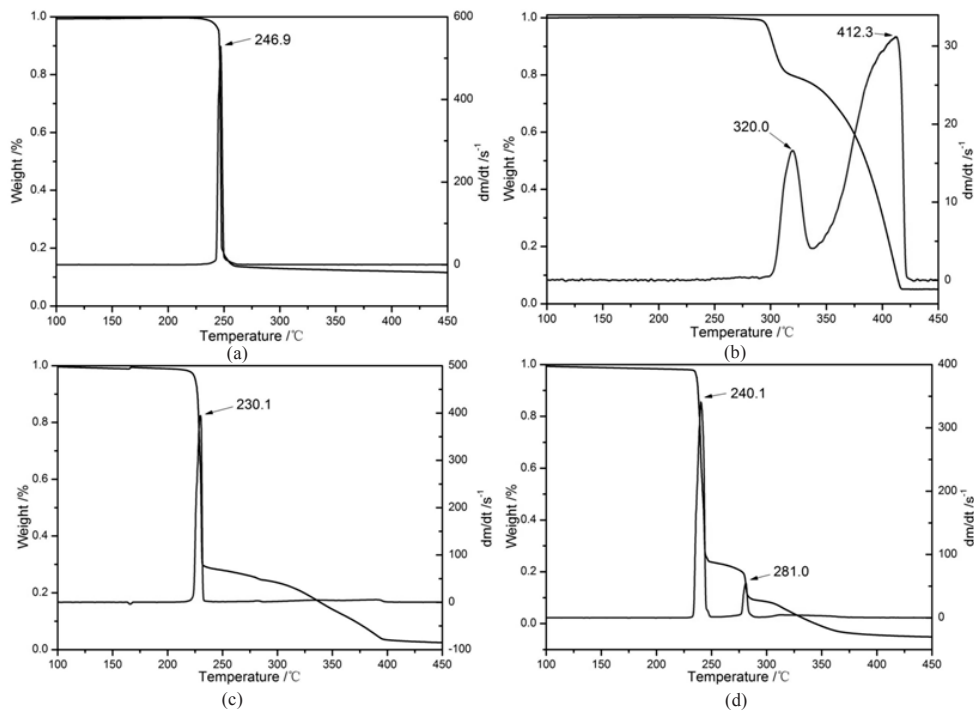


Figure 7. TG-DTG curves of (a) CL-20 (b) AP (c) CL-20/AP co-crystal and (d) mechanical mixture at molar ratio 1:1.

of co-crystal has changed a lot which proves the formation of co-crystal. In a word, the co-crystal has a special thermal decomposition performance different from both components and the mechanical mixture. The results indicate that the process of crystallisation can not only change the thermal decomposition characteristics of single components, but also give the co-crystal explosive a unique thermal decomposition behaviour.

3.6 Determination of Hygroscopic Rate

After drying for two hours in a vacuum drying oven (temperature 50 ± 5 °C), the co-crystal and raw AP were weighed 2.3 g and 1.5 g (AP contained in the same mass) respectively into a weighing bottle. The weighing bottle was placed in a constant temperature and humidity environment (temperature 40 °C, relative humidity of 75 per cent) which was achieved by putting an absorbent reactor fitted with saturated aqueous

NaCl in 40 °C water bath pot.

Every two days, the mass of both AP and co-crystal was weighed. We calculated the hygroscopic rate of each sample according to the Eqn. (1).

$$W = \frac{m_2 - m_1}{m_1} \times 100\% \quad (1)$$

where W is the mass percentage of hygroscopic rate in%. m_1 is the mass of the dry sample while m_2 is the mass of the moisture absorption one.

Figure 8 shows that the hygroscopicity of co-crystal is significantly lower than that of raw AP, in other words, the hygroscopicity of AP has been greatly reduced which is in accordance with the HMX/AP co-crystal²⁵. Through technology of co-crystal, CL-20 and AP can combine at the molecular scale level which can also change the internal composition and crystal structure of explosive. Moreover, intermolecular hydrogen bonds, due to which the stability of eutectic explosive molecular system is increased, evidently lower the hygroscopicity. So we can say that the hygroscopicity of AP is effectively reduced and the storage performance is increased by using co-crystal technology.

3.7 Possible Crystallisation Mechanism

According to the experimental data above, one can conjecture that intermolecular hydrogen bonding is the main non-covalent force during crystallisation process. Material Studio 6.1 was used to do the simulation calculation of CL-20/AP co-crystal.

The method of simulation of co-crystal structure was Polymorph Predictor (PP) and the model was based on the results of calculation surface electrostatic potential energy from DMol3. Firstly, Forcite modular was chosen to do the repeated Geometry Optimisation 5 times, Forcefield was Dreiding and the charge was use current. Then the obtained model was used to do PP calculation. The default ratio of CL-20 and AP was 1:1. Forcefield was Dreiding, the predicted space groups were P21/C, C2, P-1, P21, Pbc1 and Pna21.

It can be seen from the numerical simulation that Monte Carlo method was used to do the comprehensive statistics of density, energy, H-bond and lattice parameters of space group structures. The results of statistical analysis were as shown in Fig. 9.

Figure 9(a) reveals that the density distribution of co-crystal was 1.65 g/cm³~1.91 g/cm³, which was smaller than that of CL-20 1.92 g/cm³~2.03 g/cm³ and AP 1.95 g/cm³. Mainly because that AP molecules can't promote the densification of spaces between CL-20 molecules. Therefore, the simulation density was in the range of theoretical values. Figure 9(b) shows that the energy distribution of CL-20/AP co-crystal was 55 kcal/mol~62 kcal/mol, higher than that of CL-20(47.6 kcal/mol). Figure 9(c) shows that the H-bond energy distribution of CL-20/AP co-crystal was -6 kcal/mol ~-12 kcal/mol which

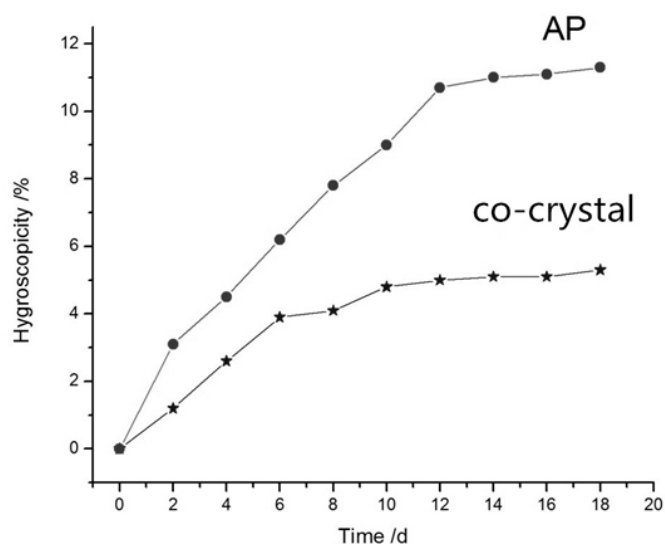


Figure 8. The change curve between hygroscopicity and time of AP and the co-crystal.

is in medium-strength range. Therefore, it is possible to form co-crystal by H-bonds under suitable conditions. Energy-density distribution in Fig. 9(d) presents a concentrated area. According to the theory of crystallography, in the process of crystallisation, the entropy decreases and the regularity of the material increases. As the degree of regularity increases, the density increases as a result. In addition, the regularity of crystal increases in the process of crystallisation accompanied by heat release. A material with lower energy can usually form a more stable crystal. Based on these two points, the energy-density optimal point was marked 'A' in Fig. 9(d). The cell parameters and structure of 'A' were presented in Table 2 and Fig. 10, respectively.

Figure 10, CL-20 and AP molecules are in a regular alternate arrangement to guarantee the maximum crystal density which provides the conditions to form hydrogen bond using the H in ammonium and further to form stable crystal structure.

4. CONCLUSIONS

- CL-20/AP co-crystal was successfully prepared by a simple solvent method at room temperature. The SEM, XRD, FT-IR Raman and DSC characterisation prove the formation of (the co-crystal, to a certain extent, also the existence of intermolecular hydrogen bonds which are the main driven forces.
- Possible crystallisation mechanism was discussed and intermolecular hydrogen bond forms are presented.
- The result of determination of hygroscopic rate indicates that the hygroscopicity of AP is effectively reduced and the storage performance is increased which may make a great contribution to military applications like propellants. Further investigation and discussion into the mechanism will be our future work.

Table 2. Cell parameters of 'A' point in Figure 9(d)

Space group	V/ Å ³	a/ Å	b/ Å	c/ Å	α /°	β /°	γ /°	ρ /g·cm ⁻³	H-bond energy/kcal·mol ⁻¹
P21/C	1929.77	21.05	12.23	22.11	90	160.18	90	1.9126	-9.3229

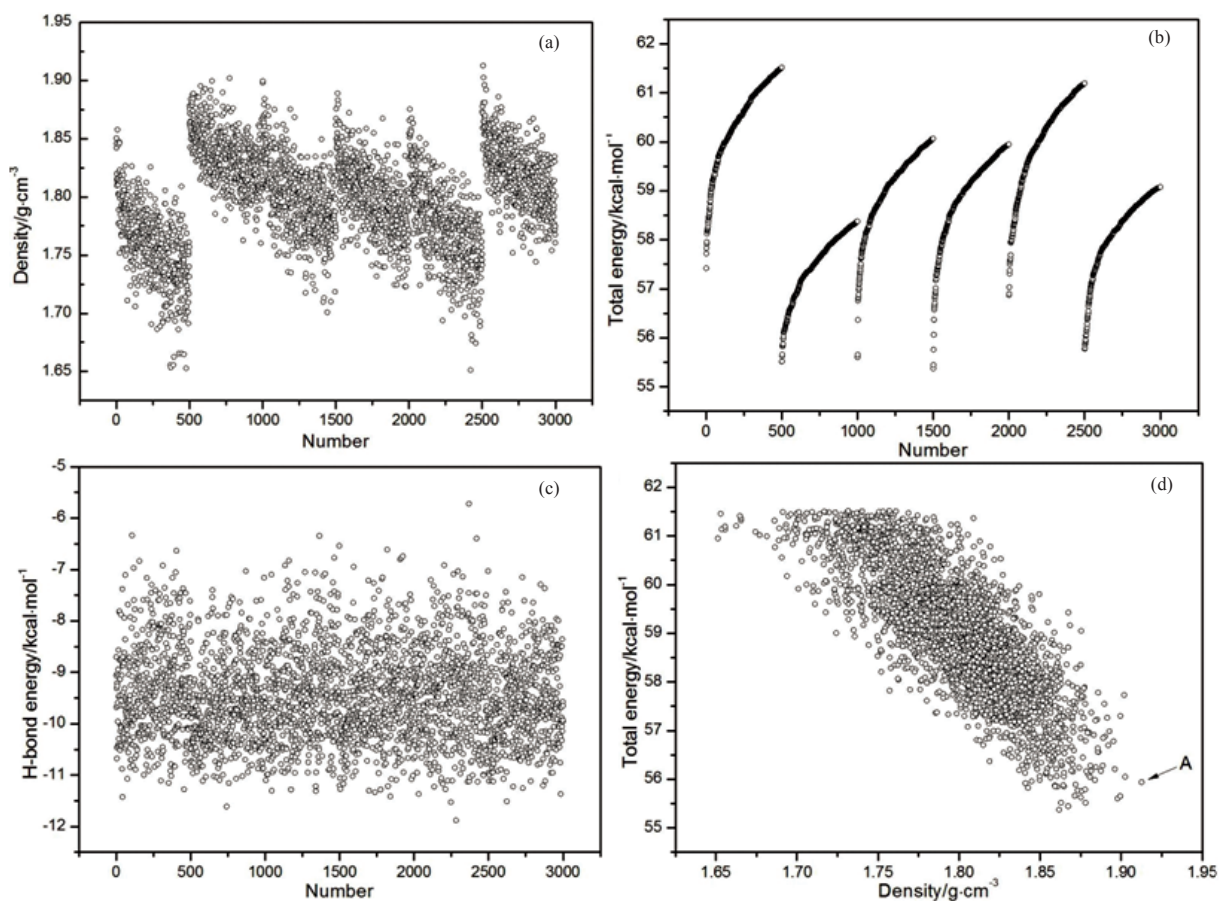


Figure 9. (a) Density distribution, (b) Energy distribution, (c) H-bond distribution, and (d) Energy-Density distribution.

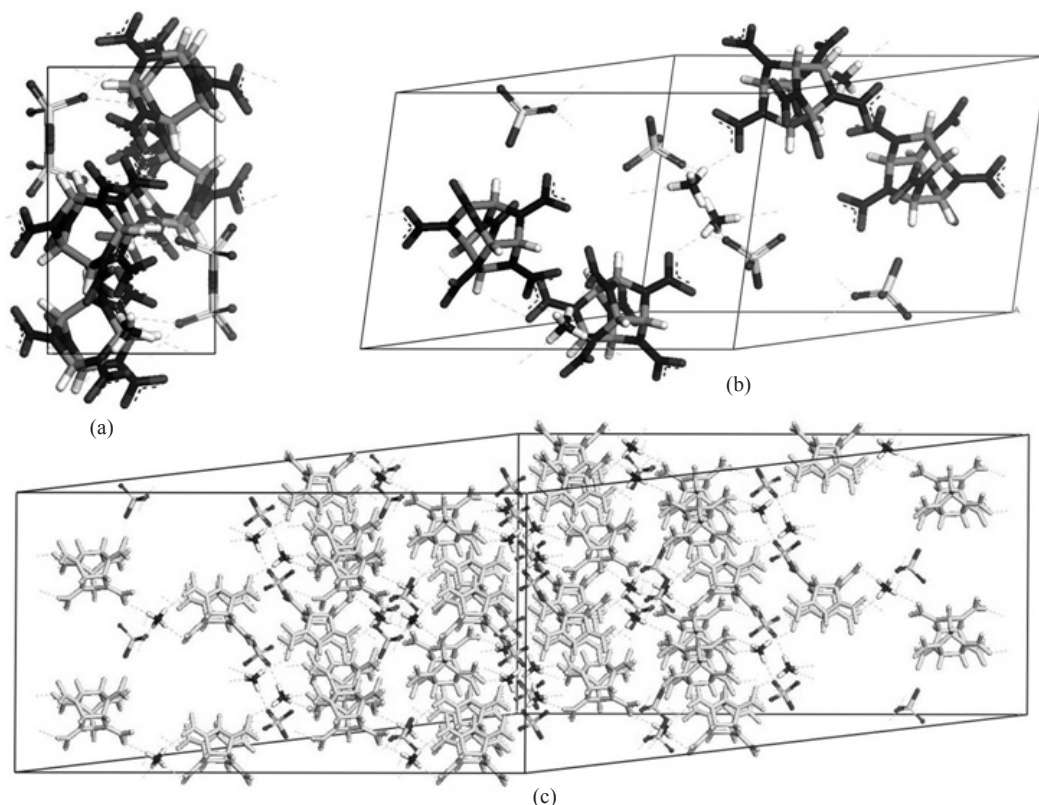


Figure 10. (a)(b) Space group structure of 'A' and (c) 2×2 supercell. (The dotted lines are H-bonds, the light colour molecules are CL-20 and the dark ones are AP in the supercell).

REFERENCES

- Trask, A.V.; Samuel, M.W.D. & William, J. Pharmaceutical cocrystallization: Engineering a remedy for caffeine hydration. *Crystal Growth Design*, 2005, **5**, 1013-1021. doi: 10.1021/cg0496540
- William, J.; Samuel, M.W.D. & Trask AV. Pharmaceutical cocrystals: An emerging approach to physical property enhancement. *MRS Bulletin*, 2006, **31**, 875-879. doi: 10.1557/mrs2006.206
- David, J. Good. & Rodríguez, H.N. Solubility advantage of pharmaceutical cocrystals. *Crystal Growth & Design*, 2009, **9**, 2252-2264. doi: 10.1021/cg801039j
- Qiao, N.; Li, M.Z.; Schlindwein, W.; Malek, N.; Davies, A. & Trappitt, G. Pharmaceutical cocrystals: An overview. *Int. J. Pharm.*, 2011, **419**(1-2), 1-11. doi:10.1016/j.ijpharm.2011.07.037
- Fleischman, S.G.; Kuduva, S.S.; McMahan, J.A.; Moulton, B.; Walsh, R.D.B.; Rodríguez-Hornedo, N. & Zaworotko, M. J. Crystal engineering of the composition of pharmaceutical phases: Multiple-component crystalline solids involving carbamazepine. *Crystal Growth Design*, 2003, **3**(6), 909-919. doi: 10.1021/cg034035x
- Schultheiss, N. & Newman, A. Pharmaceutical cocrystals and their physicochemical properties. *Crystal Growth Design*, 2009, **9**, 2950-2967. doi: 10.1021/cg900129f
- Sokolov, A.N.; Frišćić, T.; MacGillivray, L.R. Enforced face-to-face stacking of organic semiconductor building blocks within hydrogen-bonded molecular cocrystals. *J. Am. Chem. Society*, 2006, **128**(9), 2806-2807. doi: 10.1021/ja057939a
- Bolton, O.; Matzger, A.J. Improved stability and smart-material functionality realised in an energetic cocrystal. *Angewandte Chemie International Edition*, 2011, **50**, 8960. doi: 10.1002/anie.201104164
- Shen, J.P.; Duan, X.H.; Luo, Q.P.; Zhou, Y.; Bao, Q.L.; Ma, Y.J. & Pei, C.H. Preparation and characterization of a novel cocrystal explosive. *Crystal Growth Design*, 2011, **11**, 1759. doi: 10.1021/cg1017032
- Kim, K.J.; Kim, H.S. Coating of energetic materials using crystallization. *Chem. Eng. Technol.*, 2005, **28**(8), 946-951. doi: 10.1002/ceat.200500078
- Remya, S.A.O. & Mathew, S. Thermal behaviour of CuO doped phase-stabilised ammonium nitrate. *Thermochimica Acta*, 2006, **451**, 5-9. doi:10.1016/j.tca.2006.08.013
- An, C.W.; Li, F.S.; Wang, J.Y. & Guo, X.D. Surface coating of nitroamine explosives and its effects on the performance of composite modified double-base propellants. *J. Propulsion Power*, 2012, **28**(2), 444-448. doi: 10.2514/1.B34061
- Divekar, C.N.; Sanghavi, R.R.; Nair, U.R.; Chakraborty, T. K.; Sikder, A.K. & Singh, A. Closed-vessel and thermal studies on triple-base gun propellants containing CL-20. *J. Propulsion Power*, 2010, **26**(1), 120-124. doi: 10.2514/1.40895
- Yu, L.; Jiang, X. B.; Guo, X.Y.; Ren, H. & Jiao, Q.J. Effects of binders and graphite on the sensitivity of ϵ -HNIW. *J. Thermal Anal. Calorimetry*, 2012, **112**(3), 1343-1349. doi: 10.1007/s10973-012-2679-6
- Xu, S.Y.; Zhao, F.Q.; Yi, J.H.; Hu, R.Z.; Gao, H.X.; Li, S.W.; Hao, H.X. & Pei, Q. Thermal behavior and non-isothermal decomposition reaction kinetics of composite modified double base propellant containing CL-20. *Acta Physico-Chimica Sinica*, 2008, **24**(8), 1371-1377.
- Yan, Q. L.; Zeman, S. & Elbeih, A. Recent advances in thermal analysis and stability evaluation of insensitive plastic bonded explosives (PBXs). *Thermochimica Acta*, 2012, **537**, 1-12. doi:10.1016/j.tca.2012.03.009
- Samudre, S.S.; Nair, U.R.; Gore, G.M.; Sinha, R.K.; Sikder, A.K. & Asthana, S.N. Studies on an improved plastic bonded explosive (PBX) for shaped charges. *Propellants, Explosives, Pyrotechnics*, 2009, **34**(2), 145-150. doi: 10.1002/prop.200800036
- Song, X. L.; Li, F. S. Dependence of Particle size and size distribution on mechanical sensitivity and thermal stability of hexahydro-1, 3, 5-trinitro-1, 3, 5-triazine. *Def. Sci. J.*, 2009, **59**(1), 37-42.
- Song, X.L.; Wang, Y.; An, C.W.; Guo, X.D. & Li, F.S. Dependence of particle morphology and size on the mechanical sensitivity and thermal stability of octahydro-1,3,5,7-tetranitro-1,3,5,7-tetrazocine. *J. Hazardous Mater.s*, 2008, **159**(2-3), 222-229. doi:10.1016/j.jhazmat.2008.02.009
- Siviour, C.R.; Gifford, M.J.; Walley, S.M.; Proud, W.G. & Field, J.E. Particle size effects on the mechanical properties of a polymer bonded explosive. *J. Mater. Sci.*, 2004, **39**(4), 1255-1258. doi: 10.1023/B:JMSE.0000013883.45092.45
- Braga, D.; Grepioni, F. & Maini, L. The growing world of crystal forms. *Chemical Communications*, 2010, **46**, 6232-6242.
- Lara, O.F. & Espinosa, P.G. Cocrystals definitions. *Supramolecular Chemistry*, 2007, **19**, 553. doi:10.1080/10610270701501652
- Shan, N.; Zaworotko, M.J. The Role of Cocrystals in Pharmaceutical Science. *Drug Discovery Today*, 2008, **13**: 440. doi:10.1016/j.drudis.2008.03.004
- Almarsson, ö. & Zaworotko, M.J. Crystal Engineering of the Composition of Pharmaceutical phases. Do pharmaceutical co-crystals represent a new path to improved medicines? *Chemical Communications*, 2004, 1889-1896.
- Chen, J.; Duan, X.H. & Pei, C.H. Preparation and Characterization of HMX / AP Co-crystal. *Chinese J. Energetic Mater.*, 2013, **21**(4), 409-413. (Chinese)

CONTRIBUTORS

Dr Han Gao, major in energetic co-crystal materials.
Contribution in the current study, conception, methods, performed experimental part, and did statistical analysis.

Prof. Wei Jiang, major in energetic materials.
Contribution in the current study, Conception, foundations.

Dr Jie Liu, major in nano explosives.
Contribution in the current study, Foundations, methods, performed statistical analysis.

Dr Gazi Hao, major in nano energetic catalysts.
Contribution in the current study, Methods, performed experimental part and did statistical analysis.

Dr Lei xiao, major in nano explosives used in PBX.
Contribution in the current study, performed experimental and did statistical analysis.

Dr Xiang Ke, major in nano thermite.
Contribution in the current study, conception, performed experimental part.

Dr Teng Chen, major in nano energetic composites.
Contribution in the current study, performed experimental part, and did statistical analysis.